

*To be published in Optics Letters:*

**Title:** Applying light-emitting diodes with narrow-band emission features in differential spectroscopy

**Authors:** Holger Sihler, Christoph Kern, Denis Pöhler, and Ulrich Platt

**Accepted:** 25 October 2009

**Posted:** 29 October 2009

**Doc. ID:** 115221



# Applying light-emitting diodes with narrow-band emission features in differential spectroscopy

Holger Sihler,<sup>1,\*</sup> Christoph Kern,<sup>1</sup> Denis Pöhler,<sup>1</sup> and Ulrich Platt<sup>1</sup>

<sup>1</sup>*Institute of Environmental Physics, University of Heidelberg,  
Im Neuenheimer Feld 229, D-69120 Heidelberg, Germany*

*\*Corresponding author: holger.sihler@iup.uni-heidelberg.de*

Light-emitting diodes (LEDs) are a promising new type of light-source for differential optical absorption spectroscopy (DOAS). Varying differential structures in the emission spectrum of LEDs, however, display a potentially severe problem. We show that the structures, which originate from a Fabry-Pérot etalon, may be removed by tilting the emitter, which at the same time increases the radiant flux coupled into the following optical system. The results of long-path DOAS measurements, where we apply our method on a blue LED for the suppression of periodic structures, are also presented. © 2009 Optical Society of America

*OCIS codes:* 010.1280, 120.0280, 230.3670, 280.1120, 300.1030.

Differential optical absorption spectroscopy (DOAS) is a common technique used to quantify column densities and concentrations of many kinds of trace gases in the atmosphere [1]. It utilizes the characteristic narrowband absorption of trace gases with known absorption cross-sections along a light-path following the *Beer-Lambert* law. Broadband (or slowly varying) information of the final spectrum, which originates mostly from scattering processes along the light-path, is neglected.

The search for suitable sources of radiation is as old as spectroscopy itself. In the case of DOAS, either natural light sources like the sun are utilized (*passive* DOAS) or artificial light sources are part of *active* instruments. Technological progress during the last decade has made light-emitting diodes (LEDs) an interesting alternative to conventional broadband light-sources such as incandescent or arc lamps [2, 3]. In active DOAS, the application of LEDs is very advantageous with respect to power consumption, size, ease of handling, and lifetime. In fact, LEDs have already been successfully applied as light sources in long-path DOAS (LP-DOAS) measurements [4,5]. The emission spectra of most LEDs, however, exhibit strong narrowband structures which significantly increase the error of DOAS measurements

as they interfere with trace-gas absorption structures [4]. These Airy-shaped interference structures are attributed to a Fabry-Pérot etalon formed by parallel layers of refractive index contrasts within the semiconductor bulk design [6,7]. In literature, they are sometimes also called etalon-structures, interference fringes, or features of the emission spectrum.

In principle, the spectral shape of the light-source does not influence DOAS measurements, because structures cancel out when calculating the optical density  $\tau = \ln(I/I_0)$ , where  $I_0$  is the spectrum emitted by the light source and  $I$  is the spectrum after passing through absorbers in the light-path. Structures originating from the light-source only become visible in  $\tau$  if they change between  $I$  and  $I_0$ . A reason for this change may be a shift of the spectrum due to thermal and other fluctuations in the environment of the measurement, which is especially problematic for outdoor application. In case of a LED featuring strong etalon-structures, e. g. the LXHL-LR3C manufactured by Lumileds, a wavelength stability of the spectral position of the etalon-structure of  $\Delta\lambda \leq 0.01$  nm would be required in order to maintain a differential optical density of less than 0.001. We found that to meet this requirement, the temperature of the LED needs to be stabilized to  $\Delta T \leq 0.25$  K and the current to  $\Delta I \leq 6$  mA respectively.

In the past, however, the minimal detectable optical density of our LP-DOAS measurements was always dominated by etalon-structures, even though the LED was sufficiently stabilized in temperature and current. This puzzling observation was finally traced to the angular dependency of the interference structures superimposing the LED emission spectrum. Minute variations in the solid angle of LED radiation captured by the spectrometer therefore led to irreproducible changes in the integrated measurement spectrum. So far, it was not possible to achieve a sufficient stability in captured solid angle to avoid malicious structures in the calculated optical density  $\tau$ . However, the requirements regarding the stability of temperature, current and captured solid angle are reduced in case of a less structured spectrum. This work now presents a novel way to fine-tune the emission spectrum of LEDs for differential spectroscopy techniques by taking advantage of its angular dependency.

Two LED samples are studied: (1) an UVTOP340, manufactured by Sensor Electronic Technology (S-ET), emitting ultraviolet light centered at  $\lambda_0=342$  nm ( $\delta\lambda=11$  nm FWHM) and (2) a Luxeon LXHL-LR3C high-power LED, emitting blue light ( $\lambda_0=449$  nm,  $\delta\lambda=20$  nm). The active area of the UV-LED is  $0.26 \times 0.18$  mm<sup>2</sup>, which is significantly smaller than  $1 \times 1$  mm<sup>2</sup> of the blue LED. The original emission spectra of both LEDs and their highpass-filtered versions are shown in Fig. 1.

Each LED was placed on a rotary stage with the axis of rotation oriented parallel to and laying within the light-emitting surface (see inset in Fig. 2(a)). At a distance of 60 mm from the LED surface, a biconvex quartz lens ( $f=30$  mm, 19 mm aperture) was used to image the active area of the LED on a quartz fiber ( $d=100$   $\mu$ m, NA=0.22) placed at another 60 mm from

the lens. Depending on the LED type, the exit of the fiber was connected to a spectrograph entrance. In the case of the UVTOP340 LED a QE65000 spectrograph, manufactured by Ocean Optics, was used, whereas the light of the LXHL-LR3C was coupled to an Acton 500 spectrometer (equipped with a Hamamatsu S3904-1024 photo diode array detector with DOAS controller, manufactured by Hoffmann Messtechnik). Both temperature stabilized spectrographs were controlled by a PC running DOASIS version 3.2.2719 [8].

The tilt angle  $\vartheta$  between LED surface normal and optical axis was first adjusted to  $0^\circ$  (perpendicular emission) and then gradually increased. At each angle, the corresponding spectrum was obtained by averaging 100 individual scans and subtracting the appropriate offset and dark current signals. Then, the relative intensity of the spectrum was determined by integrating the intensity within the wavelength range in which it exceeded  $1/e=36.8\%$  of the maximum value at  $\vartheta = 0^\circ$ . In order to measure the strength of the etalon-structures, we introduce the maximum intensity modulation  $M$ . It is obtained by applying a combination of three filters to the spectrum: A combination of a fifth-order Savitzky-Golay and a binomial (2000 iterations) high-pass filter was applied in order to remove the broadband nature of the emission spectrum. Then, narrowband noise was removed by a binomial low-pass filter (5 iterations). Finally,  $M$  was calculated as the difference between highest and lowest value of the filtered spectrum.

Fig. 2(a) shows the angular dependency of the intensity and the modulation amplitude  $M$  for the UVTOP340.  $M$  drops from 6.7% at  $\vartheta = 0^\circ$  to a minimum of 2.5% at  $45^\circ$ . For small  $\vartheta$ , the intensity is almost constant, but then decreases to a value below 20% at  $50^\circ$ . Larger  $\vartheta$  are not evaluated here, because the LED package prevented a proper fiber coupling. In case of the LXHL-LR3C, as illustrated in Fig. 2(b),  $M$  is much larger at perpendicular emission (38%) and then decreases quickly to 5% at  $15^\circ$  and even reaches 1.2% at  $65^\circ$ . At  $60^\circ$ , the intensity amounts to 164% of the intensity at  $0^\circ$ , and only then falls off towards higher  $\vartheta$  in coincidence with an increase of  $M$ .

Two observations are emphasized here: (1)  $M$  decreases for any  $\vartheta > 0^\circ$ , and (2) the overall intensity does not drop instantly (UVTOP) or even increases (LXHL) when a tilt is applied. The same behavior was observed for a number of other commercial high-power LEDs [9]. In all experiments with devices exhibiting narrowband etalon-structures, the intensity modulation disappeared when a tilt was applied.

The decrease of  $M$  may be explained by the fact that the displacement of interfering beams increases past the coherence length ( $L_c \approx \lambda_0^2/\delta\lambda \approx 10\ \mu\text{m}$ ) of the emitted LED radiation [10]. As long as the active area of the LED is sufficiently large, the Lambertian emission pattern, which is a good approximation for planar LEDs, yields an intensity independent of  $\vartheta$ . However, as the  $M$  decreases and less radiation is reflected back into the semiconductor material, the measured intensity increases with increasing  $\vartheta$ . This increase continues until the

effective active-area of the LED becomes too small to illuminate the entire cross-section of the fiber. Then the intensity drops, an effect that occurs sooner for smaller emitters (UVTOP in Fig. 2).

Finally, in order to demonstrate the overall improvement of DOAS measurements by a tilted emitter, atmospheric LP-DOAS measurements were carried out with the LXHL-LR3C LED with two different tilt angles  $\vartheta = 0^\circ$  and  $25^\circ$ . An active DOAS instrument, as described in [11], was set up with a total light path of 6090 m across the city of Heidelberg. The LED current was  $I = (1000.0 \pm 0.1)$  mA and the temperature variations were controlled to be below 0.01 K. The light was first coupled into a single fiber (600  $\mu\text{m}$  diameter, NA=0.22) with an applied mode mixer which in turn was connected to the fiber-bundle (6+1 fibers, 100  $\mu\text{m}$ , NA=0.22) ending at the focal plane of the telescope (1.5 m focal length, 30 cm diameter). Finally, the central fiber was used to couple the transmitted light into the Acton 500 mentioned above. The optical density  $\tau$  was evaluated applying a non-linear least-square fitting algorithm, which included reference cross-sections of  $\text{NO}_2$  and  $\text{H}_2\text{O}$  in addition to a fourth-order polynomial [12].

The fit result and residual of both measurements are shown in Fig. 3. Without tilt, the amplitude of the residual is of the same order as the modeled spectrum (Fig. 3 (c)). It is dominated by the periodic etalon-structure ( $3.3 \times 10^{-2}$  optical density). The residual, obtained in the measurement with  $\vartheta = 25^\circ$ , does not contain these structures (Fig. 3 (d)). Here, the residual delta is  $5 \times 10^{-3}$  optical density. A relative  $\text{NO}_2$  measurement error of 1.6 % is derived after multiplying with a correction factor  $C=2$  [12]. Thus, the  $2\sigma$ -detection limit of the  $\text{NO}_2$  column density was estimated to  $2.1 \times 10^{15} \text{ cm}^{-2}$ . This corresponds to a mixing ratio of 0.14 ppb at the corresponding atmospheric circumstances, which is an improvement by almost one order of magnitude compared to the non-tilted case.

This example shows, that the detection limit of LP-DOAS measurements are significantly improved by tilting the LED in the fiber-coupling. The spectra could be evaluated without including any further corrections in the evaluation procedures. The achieved detection limit for  $\text{NO}_2$  is comparable to those obtained by conventional LP-DOAS instrument setups applying arc lamps as light sources (see Table 2 in [4]). This is advantageous for DOAS retrievals, because correction spectra potentially contain trace gas absorption structures. Similar improvements can be expected in measurements applying UV-LEDs, which are subject of further studies.

In conclusion, this study presents an effective way to remove apparent differential structures from the emission spectrum of light-emitting diodes, which were to date the major disadvantage of LEDs in active DOAS applications. Therefore, the requirements regarding the stability of temperature, current and especially captured solid angle of LED radiation are easier to meet compared to an unmodified setup without tilt. The influence of etalon-

structures in the DOAS evaluation could be suppressed below the noise level imposed by photon statistics. Also, other LED-applying spectroscopy techniques may benefit from a less structured emission spectrum and a higher intensity [13–17].

Published by

OSA

## References

1. U. Platt and J. Stutz, *Differential Optical Absorption Spectroscopy (DOAS) - Principles and Applications* (Springer, 2006).
2. D. A. Steigerwald, J. C. Bhat, D. Collins, R. M. Fletcher, M. O. Holcomb, M. J. Ludowise, P. S. Martin, and S. L. Rudaz, "Illumination with solid state lighting technology," *IEEE J. Sel. Top. Quant. Electron.* **8**, 310–320 (2002).
3. K. C. Kim, M. C. Schmidt, H. Sato, F. Wu, N. Fellows, M. Saito, K. Fujito, J. S. Speck, S. Nakamura, and S. P. DenBaars, "Improved electroluminescence on nonpolar *m*-plane InGaN/GaN quantum wells LEDs," *Phys. Stat. Sol. (RRL)* **1**, 125–127 (2007).
4. C. Kern, S. Trick, B. Rippel, and U. Platt, "Applicability of light-emitting diodes as light sources for active DOAS measurements," *Appl. Opt.* **45**, 2077–2088 (2006).
5. S. W. Li, P. H. Xie, W. Q. Liu, F. Q. Si, A. Li, and F. M. Peng, "A study of applicability of light emitting diodes in differential optical absorption spectroscopy measurements," *Acta Phys. Sin.* **57**, 1963–1967 (2008).
6. C. A. Tran, A. Osinski, R. F. Karlicek, and I. Berishev, "Growth of InGaN/GaN multiple-quantum-well blue light-emitting diodes on silicon by metalorganic vapor phase epitaxy," *Appl. Phys. Lett.* **75**, 1494–1496 (1999).
7. C. Hums, T. Finger, T. Hempel, J. Christen, A. Dadgar, A. Hoffmann, and A. Krost, "Fabry-perot effects in InGaN/GaN heterostructures on Si-substrate," *J. Appl. Phys.* **101**, 033113 (2007).
8. S. Kraus, *DOASIS - A Framework Design for DOAS* (Shaker, 2006).
9. J. Thieser, Max Planck Institute for Chemistry, Joh.–Joachim–Becher–Weg 27, 55128 Mainz, Germany (personal communication, 2009).
10. Y. Ohtsuka, "Optical coherence effects on a fiber-sensing Fabry-Perot interferometer," *Appl. Opt.* **21**, 4316–4320 (1982).
11. A. Merten, J. Tschritter, and U. Platt, "New design of DOAS-long-path telescopes based on fiber optics," *Appl. Opt.* , doc. ID 117759 (submitted 25 September 2009).
12. J. Stutz and U. Platt, "Numerical analysis and estimation of the statistical error of differential optical absorption spectroscopy measurements with least-squares methods," *Appl. Opt.* **35**, 6041–6053 (1996).
13. S. Ball, J. M. Langridge, and R. L. Jones, "Broadband cavity enhanced absorption spectroscopy using light emitting diodes," *Chem. Phys. Lett.* **398**, 68 (2004).
14. T. Gherman, D. S. Venables, S. Vaughan, J. Orphal, and A. A. Ruth, "Incoherent broadband cavity-enhanced absorption spectroscopy in the near-ultraviolet: application to HONO and NO<sub>2</sub>," *Environ. Sci. Technol.* **42**, 820–895 (2008).
15. F. Xu, Z. Lv, X. Lou, Y. Zhang, and Z. Zhang, "Nitrogen dioxide monitoring using a

- blue led,” *Appl. Opt.* **47**, 29 (2008).
16. J. Meinen, J. Thieser, U. Platt, and T. Leisner, “Using a high finesse optical resonator to provide a long light path for differential optical absorption spectroscopy: CE-DOAS,” *Atmos. Chem. Phys. Discuss.* **8**, 10665–10695 (2008).
  17. T. Wu, W. Zhao, W. Chen, W. Zhang, and X. Gao, “Incoherent broadband cavity enhanced absorption spectroscopy for in situ measurement of NO<sub>2</sub> with a blue light emitting diode,” *Appl. Phys. B* **94**, 58–94 (2009).

Published by  
OSA

## List of Figure Captions

Fig. 1. Intensity spectrum in arbitrary units (above) and highpass-filtered intensity modulation in % (below) of two LEDs: S-ET UVTOP340 (left) and Luxeon LXHL-LR3C (right). The highlighted area indicates the interval used to determine the relative intensity and the maximal intensity modulation  $M$ , respectively.

Fig. 2. Angular dependency of intensity (solid squares, left scale) and maximal intensity modulation  $M$  of the superimposed etalon-structures (empty circles, right scale): UVTOP340 LED (a) and Luxeon LXHL-LR3C (b). The inset in (a) illustrates the tilt between the LED emitting surface normal (solid line) and the optical axis (dashed line) by  $\vartheta$ . Errorbars are omitted for the sake of clarity.

Fig. 3. A tilt of the LED highly improves the SN-ratio of LP-DOAS measurements in which a LXHL-LR3C was applied: without (left column) and with (right column) a tilted emitter. The actual measured optical density  $\tau$  (thick line) and the total fit result (thin line) are shown in (a) and (b), respectively. The fit residual in (c) shows periodic etalon-structures which do not appear in (d). Note: (d)-ordinate is magnified by 10.

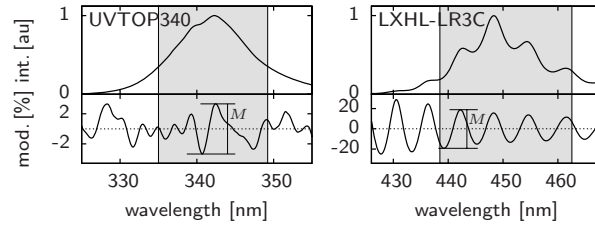


Fig. 1. Intensity spectrum in arbitrary units (above) and highpass-filtered intensity modulation in % (below) of two LEDs: S-ET UVTOP340 (left) and Luxeon LXHL-LR3C (right). The highlighted area indicates the interval used to determine the relative intensity and the maximal intensity modulation  $M$ , respectively.

Published by

OSA

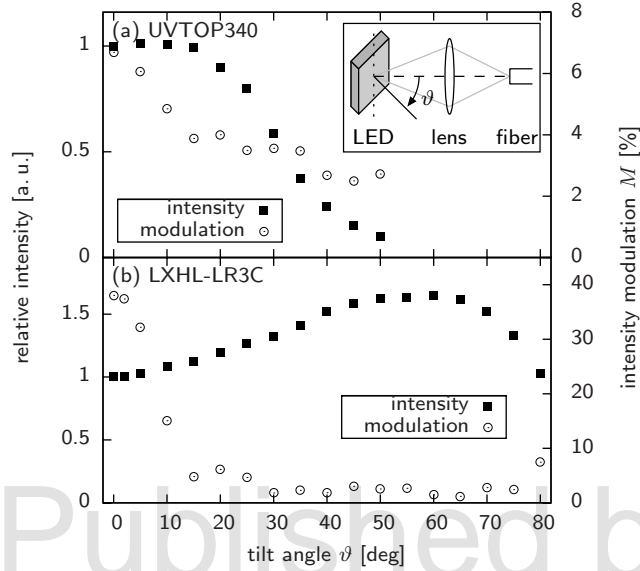


Fig. 2. Angular dependency of intensity (solid squares, left scale) and maximal intensity modulation  $M$  of the superimposed etalon-structures (empty circles, right scale): UVTOP340 LED (a) and Luxeon LXHL-LR3C (b). The inset in (a) illustrates the tilt between the LED emitting surface normal (solid line) and the optical axis (dashed line) by  $\vartheta$ . Errorbars are omitted for the sake of clarity.

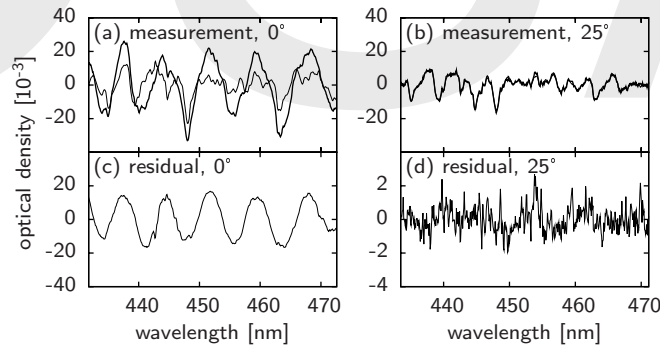


Fig. 3. A tilt of the LED highly improves the SN-ratio of LP-DOAS measurements in which a LXHL-LR3C was applied: without (left column) and with (right column) a tilted emitter. The actual measured optical density  $\tau$  (thick line) and the total fit result (thin line) are shown in (a) and (b), respectively. The fit residual in (c) shows periodic etalon-structures which do not appear in (d). Note: (d)-ordinate is magnified by 10.